Catalytic Decomposition of Nitrogen Monoxide over Valency-Controlled La_2CuO_4-Based Mixed Oxides

Hiroyuki YASUDA, Taihei NITADORI,# Noritaka MIZUNO,## and Makoto MISONO*
Department of Synthetic Chemistry, Faculty of Engineering, The University of Tokyo, Hongo, Bunkyo-ku, Tokyo 113
(Received May 25, 1993)

The direct decomposition of nitrogen monoxide (NO) to N_2 and O_2 was carried out over valency-controlled $La_{2-x}A'_xCu_{1-y}B'_yO_4$ (A'=Sr, Ba, Ca, Ce; B'=Zr, Al) mixed oxide catalysts with a K_2NiF_4-type structure. The catalysts were characterized by XRD, XPS, redox titration, and oxygen TPD. It was confirmed by XPS that the surface and bulk compositions generally agreed and by redox titration that the average oxidation number (AON) of copper varied widely from 1.60 to 2.30. XPS showed that the valency of surface copper agreed with AON for AON$\leq$2, while it was in the Cu^{2+} state for AON$>$2.0. The amounts of oxygen desorbed in TPD and the oxygen nonstoichiometry of $La_{2-x}Sr_xCuO_4$ increased with x in parallel. The catalytic activity for NO decomposition showed a maximum at $x=0.4$—0.5, and a good correlation was found between the catalytic activity and AON for all of the catalysts tested. The decomposition of dinitrogen oxide (N_2O) was also carried out for $La_{2-x}Sr_xCuO_4$ for a comparison. Based on the much slower rate of decomposition for NO than that for N_2O and the significantly high rate of oxygen TPD, it was concluded that the oxygen desorption was not the rate-determining step in the steady state. The relative activities of the catalysts studied are all well explained by a mechanism in which the active sites for NO decomposition over these catalysts are coordinatively unsaturated Cu^{2+} ions on the surface that can be easily oxidized to Cu^{3+} upon NO adsorption.

The removal of nitrogen oxides (NO_x) in the exhaust gases from automobiles and electric power plants is required for the protection of our global and local environments. The catalytic decomposition of nitrogen monoxide (NO) to N_2 and O_2 is a thermodynamically very favorable reaction below 1200 K.[1] Although various catalysts, such as metal oxide and noble metal catalysts,[2—8] have already been investigated, a practically sufficient catalytic activity has not yet been obtained, because the reaction is strongly inhibited by oxygen that is produced by decomposition or coexisting in the feed gas.[9] Nevertheless, among several denitrification processes the direct decomposition of NO is the simplest and an ideal reaction for the removal of NO_x.

Iwamoto and co-workers reported a significant catalytic activity of Cu-exchanged ZSM-5 zeolite for this reaction.[10—12] According to them, the oxidation state of copper ions is the important factor controlling the activity, and Cu^+ species, probably in the form of a Cu^+-Cu^+ dimer, are the active sites for the decomposition of NO. Li and Hall indicated that Cu–ZSM-5 became highly active when Cu^{2+} was reduced to Cu^+ by the desorption of oxygen (a rapid $Cu^{2+}\leftrightarrow Cu^+$ redox cycle).[13] Li and Armor confirmed the desorption of oxygen from Cu–ZSM-5 at about 633 K.[14] It would thus be interesting to investigate the redox property and the catalytic behavior for the decomposition of NO with a series of copper-containing catalysts in which the valency of copper is varied over a wide range.

It is possible for La_2CuO_4 to substitute a part of lanthanum and copper ions with others having different valencies, as in the case of perovskite-type mixed oxides, without affecting the fundamental structure.[15—19] As a result, the valency of copper and the nonstoichiometry of oxygen can be controlled.[20,21] For example, we previously investigated the effect of the valency of copper on the reaction between NO and CO and found that the catalysts in which the oxidation number of copper was close to two were most active.[22]

We also investigated the direct decomposition of NO over valency-controlled $La_{2-x}A'_xCu_{1-y}B'_yO_4$ catalysts and reported a good correlation between the valency of copper and the catalytic activity.[23,24] In the present study, we extended the previous work by applying various characterization methods of catalysts and increasing the variety of catalysts, in which the valency of copper was controlled systematically. We attempted to elucidate the rate-determining step of the reaction, the roles of the valency, the redox properties of copper ion, and the active sites for this reaction, and to explain based on these results the correlation between the valency of copper and the catalytic activity. We also studied the oxidation of propane over these catalysts, since a close correlation between NO decomposition and hydrocarbon oxidation is pointed out in the case of valency-controlled $LaCoO_3$ and $LaMnO_3$.[7]

Experimental

Preparation and Characterization of Catalysts. The copper-containing K_2NiF_4-type mixed oxides ($La_{2-x}A'_xCu_{1-y}B'_yO_4$) used as catalysts were prepared from metal acetates of each component in the same manner as has been described previously.[22,24] The precipitates, which had been obtained from a mixed acetate solution by evaporation to dryness, were first decomposed in air at 573 K for 1—3 h.

#Present address: Product Planning Department, Japan Tobacco Inc., Toranomon, Minato-ku, Tokyo 105.
##Present address: Catalysis Research Center, Hokkaido University, Sapporo, 060.

They were then calcined in air at 1123—1273 K for 5—20 h. The grinding was sufficiently carried out in each process for preparing catalysts. As for $La_{2-x}Sr_xCuO_4$ (x=0—1.0) catalysts, two series (calcined at 1173 and 1273 K) were prepared in order to investigate the effect of the calcination temperature. Although the actual compositions may generally be nonstoichiometric ($La_{2-x}A'_xCu_{1-y}B'_yO_{4\pm\delta}$), in the present paper they are designated by $La_{2-x}A'_xCu_{1-y}B'_yO_4$ unless the value of the nonstoichiometry (δ) is necessary.

The crystal structure was determined by powder X-ray diffraction (XRD) (Rigaku Denki, Rotaflex, RU-200) using Cu $K\alpha$ radiation. The surface areas of the samples were measured by means of the BET method (N_2 adsorption).

The average oxidation number (abbreviated by AON) of the copper in the catalysts, which was obtained by slowly cooling in air to 298 K after calcination, was determined by iodometry, as in previous papers,[22,24] according to the literature.[25,26] The oxygen nonstoichiometry was calculated on the assumption that copper was present as either a mixture of Cu^{2+} and Cu^{3+} or a mixture of Cu^{+} and Cu^{2+}, and that the other elements were La^{3+}, Sr^{2+}, Ba^{2+}, Ca^{2+}, Ce^{4+}, Al^{3+}, Zr^{4+}, and O^{2-}.

X-Ray photoelectron spectroscopy (XPS) measurements were carried out with a resolution of 0.1 eV using a JEOL JPS-90SX spectrometer and the Mg $K\alpha$ (1253.6 eV) source. The powdered samples were pressed into disks and evacuated at 298 K overnight in the spectrometer, prior to the XPS measurements. The surface composition of $La_{2-x}Sr_xCuO_4$ was calculated based on the same equation as in previous papers.[22,27] The integrated intensity of the XPS peaks of La ($3d_{5/2}$), Sr ($3d_{3/2}+3d_{5/2}$), and Cu ($2p_{3/2}$) was used for the calculation. The cross section of the photoelectron ionization was taken from the literature.[28] The binding energies were calibrated with reference to the C 1s peak (285.0 eV) resulting from carbon contamination.

Apparatus and Procedures. Catalytic Decomposition of NO: The catalytic decomposition of NO was carried out in a fixed-bed flow reactor at atmospheric pressure. A quartz glass tube (8 mm in inside diameter) was used as a reactor, and the temperature was monitored by a chromel–alumel thermocouple. The standard reaction conditions were as follows: Catalysts (1 g) were placed in the reactor and supported by quartz wool. The reactant gas was 3.17 vol% NO in He and the flow rate of the reactant gas was 30 $cm^3\ min^{-1}$. The contact time was 2.0 g s cm^{-3}. Prior to the reaction, the catalysts were usually pretreated in an O_2 stream (30 $cm^3\ min^{-1}$) for 1 h and purged by He for 10 min at 1073 K. The reactant gas was then substituted for a He stream. In some cases, although the catalysts were pretreated in a He stream (30 $cm^3\ min^{-1}$) for 2 h at 1073 K, there was no difference between the steady-state activities of the two pretreatments (see later section). For a measurement of the temperature dependence of the activity, the catalysts were cooled to 773 K in a He stream after the pretreatment, and the reactant gas was introduced. The reaction temperature was either increased or decreased stepwise in 100 K intervals from 773 to 1073 K. The reaction was carried out at each temperature for 1—3 h, until the activity became constant. The products were analyzed by gas chromatography (a molecular sieve 5A column, 1.5 m, for NO, N_2, and O_2, and a Porapak Q column, 3 m, for N_2O, both at 328 K). The activity was evaluated in terms of the conversion of NO into N_2, taking into account of the reaction of unreacted NO with the oxygen produced during the decomposition to form NO_2 (see later section).

Catalytic Decomposition of N_2O: The catalytic decomposition of dinitrogen oxide (N_2O) was also carried out in the same apparatus as the decomposition of NO. After the same pretreatment as that for the decomposition of NO, the catalysts (ca. 0.3 g) were contacted with 3.12 vol% N_2O in a He stream (60 $cm^3\ min^{-1}$). The contact time was 0.3 g s cm^{-3}. The products were analyzed by gas chromatography in the same way as for NO decomposition.

The Oxidation of Propane: The oxidation of propane was carried out at 673 K with a similar flow system. After catalysts (ca. 0.3 g) were pretreated in an O_2 stream (60 $cm^3\ min^{-1}$) for 1 h at 673 K, they were contacted with a mixture of 0.83 vol% propane, 33.3 vol% O_2, and N_2 (balance). The products were analyzed by gas chromatography (a silica gel column, 1 m, at 357 K).

Temperature Programmed Desorption (TPD) of Oxygen: TPD of oxygen was carried out with a flow system using He as a carrier gas. The oxygen impurity in the He carrier gas was removed by a molecular sieve (MS) 5A trap kept at liquid-nitrogen temperature. Prior to the run, the sample (ca. 1 g) was pretreated in an O_2 stream (30 $cm^3\ min^{-1}$) for 1 h at 1073 K and cooled to room temperature in the O_2 stream. Then the temperature of the sample was raised from room temperature to 1073 K at a constant rate of 20 $K\,min^{-1}$ in a He stream (30 $cm^3\ min^{-1}$), and the oxygen desorbed was detected by use of a quadropole mass spectrometer (NEVA, NAG-531). The reproducibility of TPD curves was confirmed for several cases by repeating the TPD run after the same pretreatments.

Results

Structures and Physicochemical Properties. The crystal structures, specific surface areas, AON (=the average oxidation numbers) of copper, and δ (=the nonstoichiometry of oxygen) for representative $La_{2-x}A'_xCu_{1-y}B'_yO_{4\pm\delta}$ (A'=Sr, Ba, Ca, Ce; B'=Al, Zr; x=0—1.0; y=0—0.2) catalysts are summarized in Table 1. $La_{2-x}A'_xCu_{1-y}B'_yO_4$(A'=Ce; B'=Al, Zr; x=0, 0.2; y=0—0.2) had the K_2NiF_4-type structure, as in the previous work,[22] except that the impurity phases were observed in some cases (see below). La_2CuO_4 and Zr-, Ce-substituted La_2CuO_4 samples were orthorhombic, while an Al-substituted sample was tetragonal. For $La_{2-x}Sr_xCuO_4$ (x=0.2—1.0) calcined at 1173 and 1273 K, the K_2NiF_4-type single phase was observed at x=0.2. However, above x=0.4, a shoulder peak at 2θ=31.5° appeared in addition to a main peak at 2θ=31.1° ((103) plane), and the peak at 31.5° became the main peak for x=1.0. Further, the (002) and (004) reflections split into two at high x values. In addition to the K_2NiF_4-type phase, small unidentified phases appeared for $La_{2-x}Ba_xCuO_4$ (x=0.4—0.5) and $La_{1.5}Ca_{0.5}CuO_4$. Sr-, Ba-, and Ca-substituted samples were all tetragonal.

The AON of copper and δ for $La_{2-x}A'_xCuO_{4\pm\delta}$ (A'=Sr, Ba, Ca; x=0—1.0) are shown in Fig. 1 as a function

Table 1. Structures, Specific Surface Areas, the Average Oxidation Numbers (AON) of Copper, and δ of $La_{2-x}A'_xCu_{1-y}B'_yO_{4\pm\delta}$

Catalyst	Calcination Temp / K	Calcination Time / h	Structure	Surface area / $m^2\ g^{-1}$	AON of copper	δ
$La_2Cu_{0.8}Zr_{0.2}O_4$	1123	5	K[a](O[b])+ZrO_2 (8%) $La_2Zr_2O_7$(tr.[b])	10.5	1.60	−0.04
$La_2Cu_{0.9}Zr_{0.1}O_4$	1123	5	K(O)	7.7	1.84	−0.03
$La_2Cu_{0.8}Al_{0.2}O_4$	1123	5	K(T[b])+$LaAlO_3$(tr.)	2.2	1.88	−0.05
$La_{1.8}Ce_{0.2}CuO_4$	1123	5	K(O)+CeO_2(16%)	2.8	1.97	−0.09
La_2CuO_4	1173	20	K(O)	0.5	2.00	0.00
$La_{1.8}Sr_{0.2}CuO_4$	1173	20	K(T)	1.3	2.20	0.00
$La_{1.5}Sr_{0.5}CuO_4$	1273	5	K(T)+K′[c](tr.)	0.9	2.30	0.10
$LaSrCuO_4$	1273	20	K(T)+K′[c](182%)	1.0	2.21	0.39
$La_{1.8}Ba_{0.2}CuO_4$	1173	20	K(T)	0.8	2.20	0.00
$La_{1.8}Ca_{0.2}CuO_4$	1173	20	K(T)	0.6	2.10	0.05

a) K: K_2NiF_4-type structure. b) O: Orthorhombic, T: Tetragonal; Figures in parentheses are the ratios of main peak intensities of the impurities to those of the main phases; tr.: Trace is less than 3%. c) K′: K_2NiF_4-type related structure (see the text).

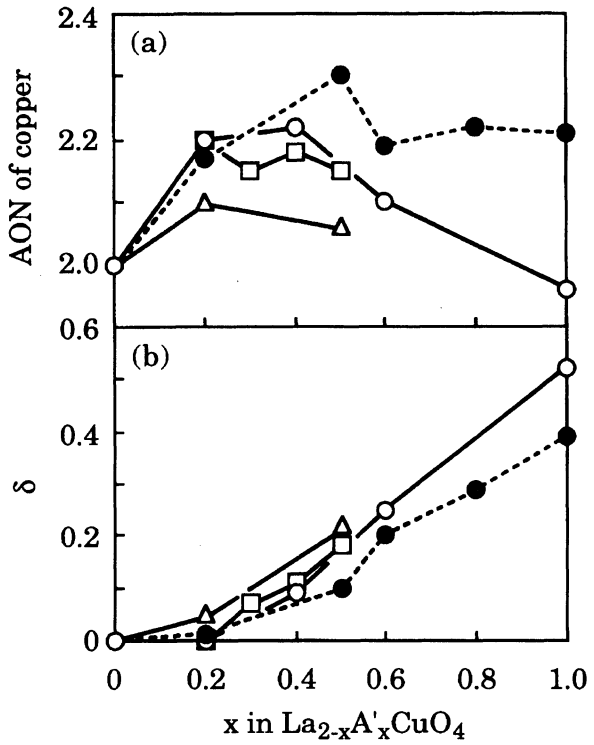

Fig. 1. Average oxidation numbers (AON) of copper and the nonstoichiometry of oxygen (δ) of $La_{2-x}A'_xCuO_{4-\delta}$. (a) AON, (b) δ. ●: $La_{2-x}Sr_xCuO_4$ (1273 K calcination), ○: $La_{2-x}Sr_xCuO_4$ (1173 K calcination), □: $La_{2-x}Ba_xCuO_4$, △: $La_{2-x}Ca_xCuO_4$.

of the extent of substitution, x. In all cases, the AON of copper increased upon substitution at the A-site up to 10—20 % ($x \leq 0.2$) (Fig. 1a). The increase in the valency was very small for Ca-substituted catalysts. On the other hand, δ increased with an increase of x above $x=0.2$ (Fig. 1b).

As shown in Table 1, both the AON of copper and δ were widely varied from 1.60 to 2.30, and from −0.09 to 0.52, respectively. The oxidation number higher than two is due to the presence of either Cu^{3+} or pairs of Cu^{2+} and a positive hole according to the literature.[29]

Surface Compositions of Catalysts. As shown in Fig. 2 and Table 2, the binding energies of Cu $2p_{3/2}$ in $La_{2-x}Sr_xCuO_4$ (x=0—1.0) samples calcined at 1273 K showed little change from $x=0$ to $x=1.0$ (between 934.3 eV ($x=1.0$) and 934.6 eV (x=0.2, 0.6)), although the valency of copper in the bulk varied from 2.00 to 2.30. The I_{sat}/I_{main} ratios (I_{main} and I_{sat} are the peak intensities of the main and satellite signals of Cu $2p_{3/2}$, respectively) for $La_{2-x}Sr_xCuO_4$ are between 0.50 and 0.58. These values agreed in general with that reported for CuO (0.53).[30] Only one L_3VV Auger peak assignable to Cu^{2+} (ca. 918 eV)[31] was observed for $La_{2-x}Sr_xCuO_4$.

The surface compositions of the metallic elements of $La_{2-x}Sr_xCuO_4$ are summarized in Table 2, together with those for the bulk. The surface compositions of Cu were close to the bulk compositions for $x \leq 0.4$, while they were slightly greater on the surface for x=0.6—1.0. The surface Sr content agreed well with the bulk content.

A similar trend with respect to the binding energy of Cu $2p_{3/2}$ and the surface compositions was obtained for $La_{2-x}Sr_xCuO_4$ samples calcined at 1173 K, as well.

The Effects of Substitution at A-Site on the Catalytic Decomposition of NO. $La_{2-x}A'_xCu_{1-y}B'_yO_4$ catalysts showed the activity for the decomposition of NO above 773 K, and the activity increased with an increase in the temperature. Hereafter, the results for $La_{2-x}Sr_xCuO_4$ catalysts calcined at 1173 K will be described unless otherwise stated. N_2O formed over Sr- and Ba-substituted catalysts below 873 K; the amount was higher at lower temperatures (the highest selectivity to N_2O was 41 % at 773 K and $x=0.6$

Table 2. Binding Energies (BE) and I_{sat}/I_{main} Ratios of Cu $2p_{3/2}$, and Surface Compositions for $La_{2-x}Sr_xCuO_4$ (1273 K Calcination) by XPS

Catalyst	BE	I_{sat}/I_{main}[a)]	Composition					
			Surface[b)]			Bulk[c)]		
	eV		La	Sr	Cu	La	Sr	Cu
La_2CuO_4	934.4	0.53	0.66		0.34	0.67		0.33
$La_{1.8}Sr_{0.2}CuO_4$	934.6	0.50	0.56	0.07	0.37	0.60	0.07	0.33
$La_{1.5}Sr_{0.5}CuO_4$	934.5	0.54	0.46	0.17	0.36	0.50	0.17	0.33
$La_{1.4}Sr_{0.6}CuO_4$	934.6	0.57	0.41	0.21	0.39	0.47	0.20	0.33
$La_{1.2}Sr_{0.8}CuO_4$	934.4	0.56	0.37	0.22	0.41	0.40	0.27	0.33
$LaSrCuO_4$	934.3	0.58	0.32	0.24	0.44	0.33	0.33	0.33

a) I_{main} and I_{sat} are the peak intensities of the main and satellite signals of Cu $2p_{3/2}$, respectively. b) Calculated by XPS peak intensity using the integrated areas of the La $3d_{5/2}$, Cu $2p_{3/2}$, and Sr ($3d_{3/2}+3d_{5/2}$). c) Calculated from the quantity of the starting materials of preparation.

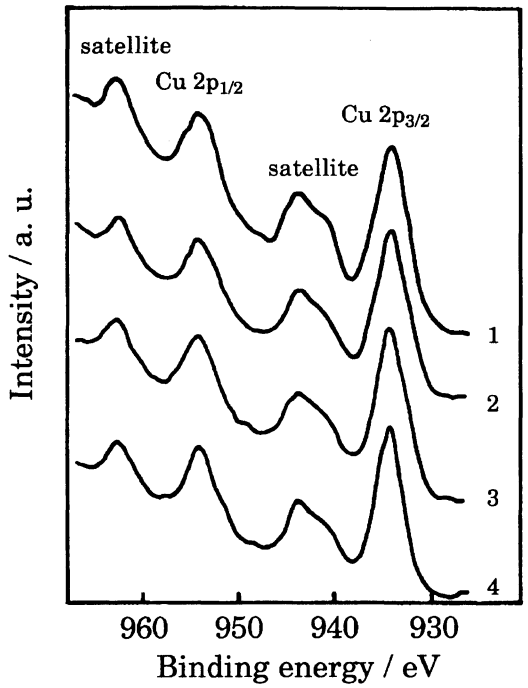

Fig. 2. XPS spectra of Cu 2p peaks. Spectra 1,2,3, and 4 correspond to those of La_2CuO_4, $La_{1.8}Sr_{0.2}CuO_4$, $La_{1.4}Sr_{0.6}CuO_4$, and $LaSrCuO_4$, respectively.

for Sr-substituted catalysts, and 44 % for $x=0.2$ of Ba-substituted catalysts). However, N_2O was not detected above 973 K. The % conversion of NO over $La_{1.6}Sr_{0.4}CuO_4$ at 973—1073 K was measured under several reaction conditions at the same W/F (2.0 g s cm^{-3}): one was at W (the catalyst weight)=1 g and F (the flow rate of the reactant)=30 cm^3min^{-1}, and another at $W=2$ g and $F=60$ cm^3 min^{-1}. There was no difference in the conversion of NO between the two cases. Thus, the diffusion in boundary layers was not rate-limiting under the present condition.[24)] It was noted that the % conversion decreased when the flow rate was further lowered to 15 cm^3 min^{-1}. In the catalytic decomposition of NO, the amount of NO converted was not equal to the amounts of N_2 and O_2 analyzed by gas chromatograph. The reason for this discrepancy is due to the reaction between the O_2 produced and the unreacted NO, that is, $NO+1/2\ O_2 \rightarrow NO_2$, in the cold part after the catalyst bed, as previously demonstrated.[32)] Also, in the present study the nitrogen (and oxygen) balance was 100±2 % when it was calculated by assuming the above reaction, thus confirming that the decomposition of NO proceeded catalytically.

The rate was very reproducible when the reaction temperature was changed up and down. The activity of $La_{1.4}Sr_{0.6}CuO_4$, which was relatively high, did not change for at least 30 h, and no changes in the crystal structure before and after the reaction were detected by XRD. The pressure dependence of the reaction rate (NO: 1.09—3.17 vol%) is shown for $La_{1.6}Sr_{0.4}CuO_4$ in Fig. 3 (○). The 1.1—1.2 order with respect to NO was indicated at 973—1073 K, in general agreement with those reported for Cu–ZSM-5.[10)]

The effects of the Sr^{2+}, Ba^{2+}, and Ca^{2+} substitutions at the A-site of La_2CuO_4 (1073 K) are shown in Fig. 4a. Upon Sr substitutions, the catalytic activity initially increased, reached a maximum at $x=0.4$ (1173 K calcination) or 0.5 (1273 K calcination), and then decreased upon further substitutions. The activity also increased for Ba substitutions. On the other hand, the effect of Ca substitutions was much smaller. The activity was thus in the order Ba>Sr>Ca for $x\leq 0.2$, where all of these catalysts had a single phase of the K_2NiF_4-type structure.

The catalytic activities of $La_{2-x}Sr_xCuO_4$ for propane oxidation at 673 K are shown in Fig. 4b. The activities were much lower than those of $LaCoO_3$,[33)] and the effect of Sr substitution was not remarkable, in contrast to the case of the decomposition of NO.

The Influence of Oxygen on the Catalytic Decomposition of NO. In order to investigate the influence of the oxidation state of the surface layers on the decomposition of NO, the catalyst was pretreated in different ways. When a reactant gas (1.02 vol% NO in He) was introduced onto $La_{1.4}Sr_{0.6}CuO_4$ (1273 K calci-

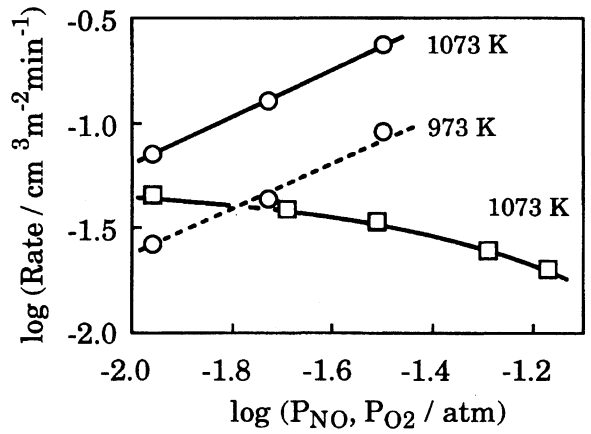

Fig. 3. Dependence of the rate of NO decomposition on the pressure of NO and oxygen for $La_{1.6}Sr_{0.4}CuO_4$ (1173 K calcination). ○: NO at 0.0109—0.0317 atm, □: oxygen at 0.0110—0.0683 atm.

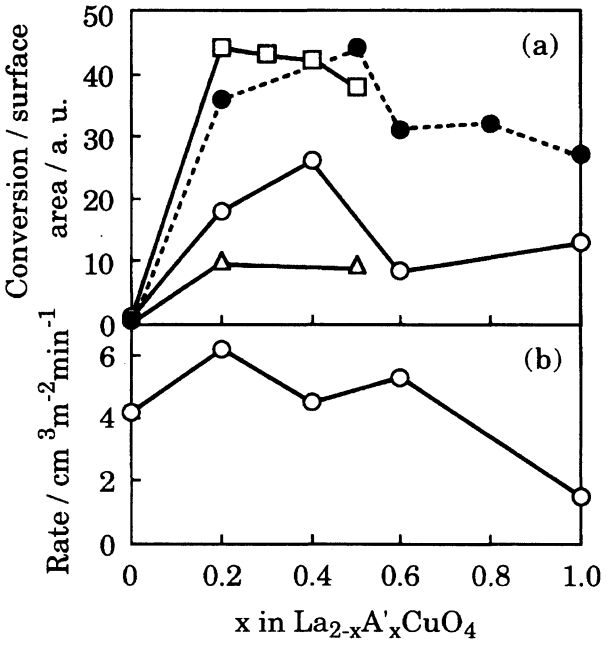

Fig. 4. Catalytic activities of $La_{2-x}A'_xCuO_4$ for NO decomposition at 1073 K (a) and those of $La_{2-x}Sr_xCuO_4$ for propane oxidation at 673 K (b). ●: $La_{2-x}Sr_xCuO_4$ (1273 K calcination), ○: $La_{2-x}Sr_xCuO_4$ (1173 K calcination), □: $La_{2-x}Ba_xCuO_4$, △: $La_{2-x}Ca_xCuO_4$.

nation) at 1073 K after it had been pretreated in a He stream for 2 h at 1073 K, the conversion was initially high, but decreased and the rate became constant after 1 h, as shown in Fig. 5a (○). The mass balances of nitrogen and oxygen during the initial stage indicated that a part of the oxygen produced from NO was consumed for the oxidation of catalyst. On the other hand, when the catalyst was pretreated in an O_2 stream for 1 h at 1073 K, after the conversion initially increased slightly, the rate became constant (Fig. 5a (□)). As a result, the steady-state activities for both pretreatments

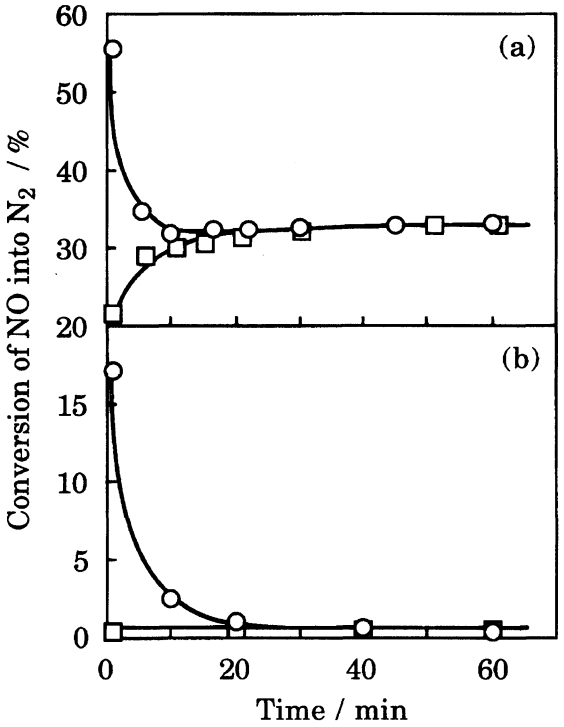

Fig. 5. Effects of pretreatments on the catalytic activities for NO decomposition. (a) NO decomposition over $La_{1.4}Sr_{0.6}CuO_4$ (1273 K calcination) at 1073 K. ○: He pretreatment for 2 h at 1073 K, □: oxygen for 1 h at 1073 K. (b) NO decomposition over $La_{1.6}Sr_{0.4}CuO_4$ (1173 K calcination) at 773 K. ○: He pretreatment for 2 h at 1073 K, □: He for 10 min at 773 K.

became equal.

Similar results were obtained for $La_{1.6}Sr_{0.4}CuO_4$ at 773 K, as shown in Fig. 5b. In this case the catalyst was preheated at 1073 K in a He stream (○) or preheated in He only to 773 K (□). The conversion at steady state was as low as 0.5 % at 773 K.

The influence of oxygen coexisting in the feed gas was also examined during the steady-state decomposition of NO. The results are shown in Fig. 3 (□). The activity decreased significantly in the presence of oxygen. The reaction order with respect to O_2 was -0.5 ± 0.25 order in the range of 1.1—6.8 vol%.[24]

TPD of Oxygen. Figure 6 shows the TPD profiles of oxygen from $La_{2-x}Sr_xCuO_4$ calcined at 1173 K, where the rates of desorption are calculated from the oxygen concentration in the eluent gas. The oxygen started to desorb at a low temperature (333 K) for La_2CuO_4, but diminished rapidly. As for the Sr-substituted samples, the oxygen began to desorb at 473—553 K, and the amounts of oxygen desorbed up to 1073 K, as well as the rates of desorption above 773 K, increased monotonically with an increase in the Sr content ($x \geq 0.2$).

The amounts of oxygen desorbed below 1073 K, expressed in units of the surface layer and in the change

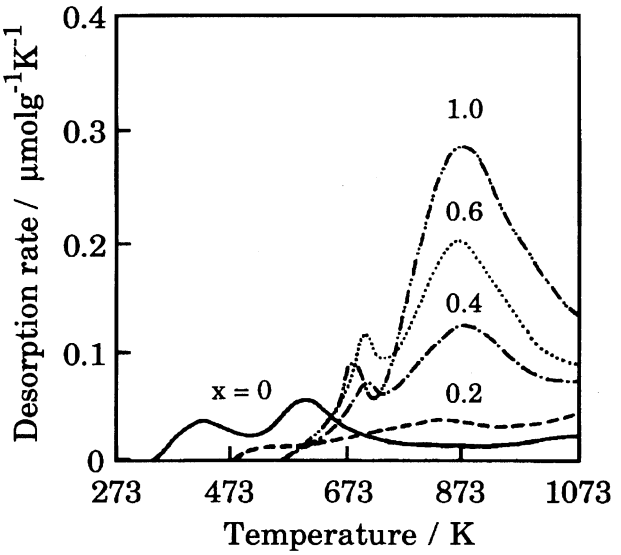

Fig. 6. TPD profiles of oxygen from $La_{2-x}Sr_xCuO_4$ (1173 K calcination).

of the oxygen nonstoichiometry, are shown in Table 3. The amount in units of the surface layer is defined by the ratio of the amount of oxygen desorbed to the amount of oxygen corresponding to the surface monolayer, where the surface density of oxygen was assumed to be 0.96×10^{19} atom m^{-2} as in previous papers.[18,19] The change in the nonstoichiometry is shown by $\Delta\delta$ in $La_{2-x}Sr_xCuO_{4-\delta-\Delta\delta}$. Both values increased monotonically up to x=1.0 along with an increase in x. The former exceeded unity (greater than monolayer) above x=0.4, showing that the desorption of lattice oxygen from the catalyst bulk occurred, in addition to the adsorbed oxygen. However, the amounts were much smaller than those observed for $La_{1-x}Sr_xCoO_3$ (x=0.2—0.6).[34]

Catalytic Decomposition of N_2O. The temperature dependences of the decomposition of N_2O and NO over $La_{1.6}Sr_{0.4}CuO_4$ are shown in Fig. 7. The catalytic activity for N_2O decomposition appeared above 673 K, and the conversion reached 100 % at 873 K. The N_2O decomposition is much faster than the NO decomposition when compared under the same conditions.

The changes in the reaction rate upon the addition of NO (2 vol%) to the feed of N_2O (1 vol%) at the steady-state reaction are shown in Fig. 8. The circles in Fig. 8 are the % conversions of N_2O calculated from the decrease in the N_2O concentration, and the squares the % conversions to N_2 from N_2O and NO (calculated from the N_2 concentration). The agreement between the two values indicates that the nitrogen balance for the decomposition of N_2O was established and only the N_2O decomposition proceeded, that is, the NO decomposition did not occur. Although the conversion of N_2O decreased upon the addition of NO at 773 K and 873 K, the decomposition of N_2O took place to a certain extent under the conditions where NO did not decompose at all. The activity for the N_2O decomposition

Table 3. Amounts of Oxygen Desorbed in TPD, the Corresponding Layers, and the Change of the Nonstoichiometry for $La_{2-x}Sr_xCuO_4$ (1173 K Calcination)

Catalyst	Amount of O_2 desorbed[a]		
	10^{-5} mol g^{-1}	Layers[b]	$\Delta\delta$[c]
La_2CuO_4	0.74	0.9	0.006
$La_{1.8}Sr_{0.2}CuO_4$	0.70	0.7	0.005
$La_{1.6}Sr_{0.4}CuO_4$	1.72	1.8	0.013
$La_{1.4}Sr_{0.6}CuO_4$	2.58	2.7	0.019
$LaSrCuO_4$	3.39	3.9	0.023

a) The amounts of oxygen desorbed in 298—1073 K. b) The surface layers corresponding to the amount of oxygen desorbed. c) The change of the nonstoichiometry owing to the oxygen desorption during TPD experiments.

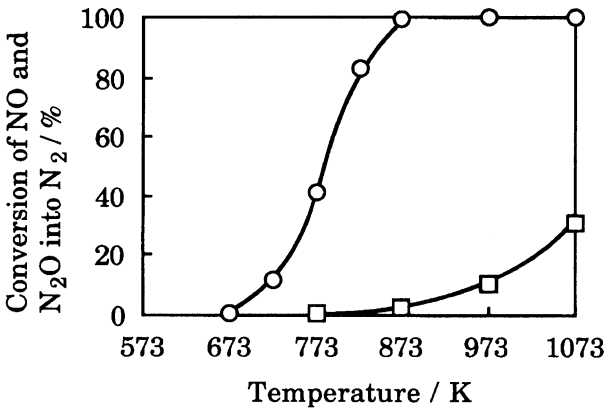

Fig. 7. Temperature dependence of the conversion of N_2O and NO into N_2 for $La_{1.6}Sr_{0.4}CuO_4$ (1173 K calcination). ○: conversion of N_2O, □: conversion of NO into N_2.

recovered within a short period when the supply of NO was stopped.

Relationship between Valency of Copper and Catalytic Activity. The activities of $La_{2-x}A'_xCu_{1-y}B'_yO_{4\pm\delta}$ catalysts for the decomposition of NO at 1073 K are plotted against the AON (=the average oxidation numbers) of copper and δ (=the nonstoichiometry of oxygen) in the bulk of catalysts in Fig. 9, in which the data reported in the previous work[24] are included. The activity was represented by the % conversion of NO into N_2 divided by the specific surface area relative to that for La_2CuO_4. A similar trend was obtained for the activity per weight of catalyst as well, since the change of surface areas were relatively small.

As shown in Fig. 9a, a good correlation between the AON of copper in the bulk and the catalytic activity was confirmed (see, also Fig. 1 and Fig. 4): The activity increases with an increase in the AON (Fig. 9a), while the correlation between δ and the activity is poor (Fig. 9b). Although the AON of copper before use for the reaction was used in Fig. 9, it was almost unchanged, even under the reaction conditions, as discussed in a later section.

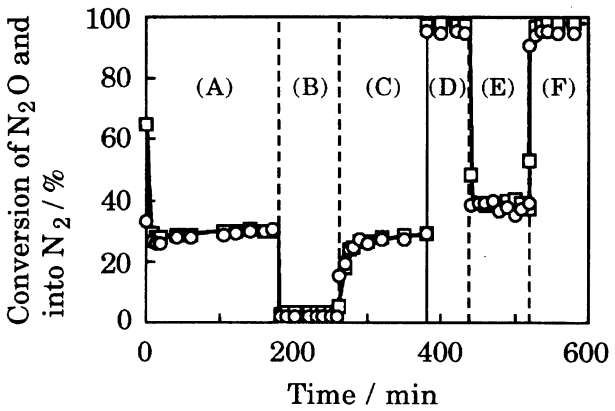

Fig. 8. Effects of coexisting NO on the conversion of N_2O for $La_{1.6}Sr_{0.4}CuO_4$ (1173 K calcination) at W/F=0.3 g s cm^{-3}. (A), (C): 1 vol% N_2O in He at 773 K, (B): 1 vol% N_2O and 2 vol% NO in He at 773 K, (D), (F): 1 vol% N_2O in He at 873 K, (E): 1 vol% N_2O and 2 vol% NO in He at 873 K. ○: conversion of N_2O, □: conversion into N_2.

The same activity data are plotted in a linear scale in Fig. 10. Essencially the same trends are noted.

Discussion

The Bulk Structure and Valency of Copper of $La_{2-x}A'_xCuO_4$ Catalysts. Nguyen et al.[35] reported that the K_2NiF_4-type structure was obtained over a wide range, $0 \leq x \leq 1.34$, for $La_{2-x}Sr_xCuO_4$ calcined at 1273—1473 K. In the present study, we confirmed the formation of the K_2NiF_4-type single phase in the range $0 \leq x \leq 0.2$. The differences in the range may be due to the lower calcination temperature (1173—1273 K) in the present study. The change observed for $x \geq 0.4$ in the XRD pattern is presumably due to the formation of a subcell derived from a tetragonal K_2NiF_4-type structure, which has the ordering of oxygen vacancies, as reported by Nguyen et al. It is possible for $x=1.0$ that the $SrLaCuO_4$ phase reported by Goodenough et al.[36] was formed.

As shown in Table 1 and Fig. 1, the AON of copper was 2.00 for La_2CuO_4, and became greater than two upon Sr, Ba, and Ca substitution at the A-site. Note that AON mainly reflects the catalyst bulk, since most copper ions are in the bulk. The change in the AON is explained by the following two equations, similarly to the cases of perovskite-type oxides, where $A'=Sr^{2+}$, Ba^{2+}, and Ca^{2+}:[33]

$$La_2CuO_4 \rightarrow La_{2-x}A'_xCu^{2+}_{1-x}Cu^{3+}_xO_4 \quad (1)$$

$$La_{2-x}A'_xCu^{2+}_{1-x}Cu^{3+}_xO_4 \rightarrow La_{2-x}A'_xCu^{2+}_{1-x+2\delta}Cu^{3+}_{x-2\delta}O_{4-\delta} + \delta/2\ O_2 \quad (2)$$

Table 1 and Fig. 1 show that upon a small extent of Sr^{2+} substitution ($x \leq 0.2$) the balance of the charge, or the electroneutrality, is maintained by the formation of Cu^{3+} according to Eq. 1, while for a high extent of substitution ($x \geq 0.4$) δ starts to increase according to Eq. 2. The valency control of copper according to Eq. 1 is more favored for catalysts calcined at 1273 K than those at 1173 K, probably due to an improvement of the crystallinity.

The proportions of Eqs. 1 and 2 must be determined by the balance between the unstability of the Cu^{3+} ion compared to Cu^{2+}, and the stability of the K_2NiF_4-type structure. The decrease in the concentration of Cu^{3+} for $x \geq 0.6$ is thus due to the fact that an oxygen-deficient structure becomes more stable for high x values by an ordering of the oxygen defect or a modification of the structure, as reported in the literature.[35]

The tolerance factor for A_2BO_4-type oxides is defined by the following equation:[37]

$$t = r(\text{A–O})/\sqrt{2}\cdot r(\text{B–O}), \quad (3)$$

where r(A–O) and r(B–O) are the atomic distances calculated based on the ionic radii.[38] The stability of tetragonal or orthorhombic structures can be estimated by the t values. For example, the tetragonal K_2NiF_4-type structure is usually stable over the range $1.02 > t > 0.85$. The t values for $La_{1.8}A'_{0.2}CuO_4$ are 0.863 (A'=Ba), 0.852 (Sr), and 0.847 (Ca). Hence, the stability of these mixed oxides would be in the order Ba> Sr>Ca, that is, the order of the tolerance factor. The more stable the K_2NiF_4-type structure is (Ba>Sr>Ca) (or the greater the lattice energy is), the stoichiometric K_2NiF_4-type structure could be maintained even with large amount of Cu^{3+} ion. In other words, the formation of the oxygen defects (Eq. 2) would become more difficult and the valency control according to Eq. 1 would prevail more in the order Ba>Sr>Ca (greater concentration of Cu^{3+}). This expectation is consistent with the present result shown in Table 1; for $x=0.2$, AON of copper is 2.10 ($\delta=-0.05$) for Ca, and 2.20 for Ba and Sr ($\delta=0.00$).

Surface Composition and Cu Valency of $La_{2-x}Sr_xCuO_4$. The surface compositions of the metallic elements of $La_{2-x}Sr_xCuO_4$ generally agreed with the bulk compositions (Table 2). The surface properties therefore seem to well reflect those of the bulk.

The oxidation states of copper on the surface of $La_{2-x}A'_xCu_{1-y}B'_yO_4$ can be estimated from the I_{sat}/I_{main} ratio of Cu $2p_{3/2}$ and Cu L_3VV Auger peak, as described in a previous paper.[22] It is known for the Cu 2p peaks that Cu^+ shows no satellite peaks in XPS, while Cu^{2+} has intense satellite peaks.[39,40] The oxidation numbers of copper estimated by the ralative intensity of the satellite peak are in general agreement with those in the bulk, when the AON is below or equal to two, as in the previous work.[22] However, a disagreement was found when the AON was higher than two; the oxidation number of copper on the surface was two despite of higher values in the bulk.

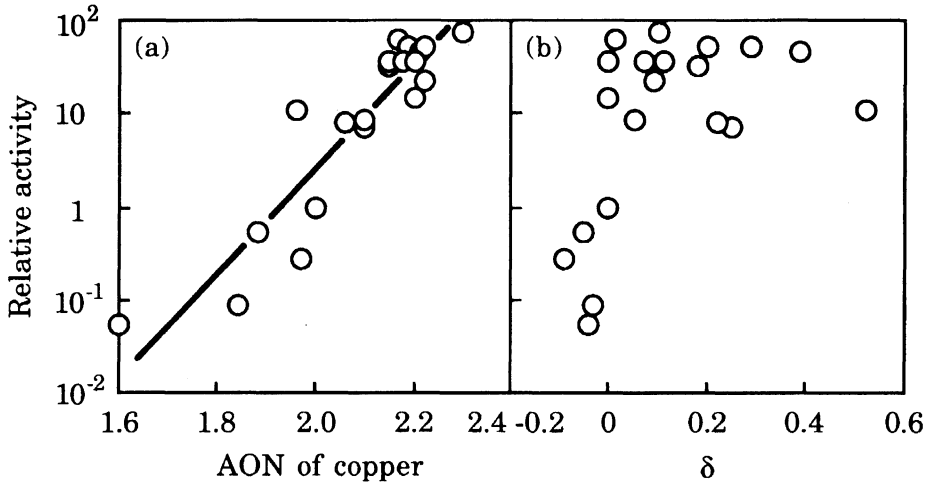

Fig. 9. Correlation between the catalytic activities of NO decomposition (1073 K) in log scale and average oxidation numbers (AON) of copper (a) or the nonstoichiometry of oxygen (δ) (b) for $La_{2-x}A'_xCu_{1-y}B'_yO_{4\pm\delta}$ (A'=Sr, Ba, Ca, Ce; B'=Zr, Al; x=0—1.0; y=0—0.2). Relative activity: the activity represented by the % conversion of NO into N_2 divided by the specific surface area relative to that for La_2CuO_4.

The binding energies of Cu $2p_{3/2}$ were between 934.3 eV (x=1.0) and 934.6 eV (x=0.2, 0.6). Steiner, et al.[41] reported that the Cu $2p_{3/2}$ peak of XPS assigned to Cu^{3+} for $NaCuO_2$ was located at about 1.3 eV higher than that of Cu^{2+} in La_2CuO_4 and CuO. In the present study, no significant chemical shifts attributable to the presence of Cu^{3+} were observed, and the I_{sat}/I_{main} ratios of Cu $2p_{3/2}$ and the kinetic energies of CuL_3VV Auger peak were close to the values reported for CuO.[30,31] Therefore, it is very probable that the oxidation number of copper on the surface is two, even when that in the bulk is greater than two. Cu^{3+} (or positive hole on oxide) may not be stable on the surface, and tends to be Cu^{2+} due to a partial desorption of oxygen in the surface layer.[42]

The Rate-Determining Step of the NO Decompostion. NO and N_2O decomposition may be considered based on the following three steps: adsorption of the reactant (NO or N_2O) (Eqs. 4 and 7), its dissociation and desorption of nitrogen (Eqs. 5 and 8), and desorption of oxygen (Eqs. 6 and 9), as has generally been assumed in the literature.[2,12,43—46]

For NO :

$$2NO \rightarrow 2NO(ad) \quad (4)$$

$$2NO(ad) \rightarrow 2O(ad) + N_2 \quad (5)$$

$$2O(ad) \rightarrow O_2 \quad (6)$$

For N_2O :

$$N_2O \rightarrow N_2O(ad) \quad (7)$$

$$N_2O(ad) \rightarrow O(ad) + N_2 \quad (8)$$

$$2O(ad) \rightarrow O_2 \quad (9)$$

Since the desorption of adsorbed oxygen atoms as an oxygen molecule (Eqs. 6 and 9) is a common step for both reactions, if this step is rate-determining, the decomposition of NO and N_2O should proceed at the same rate, provided that the catalyst surface is in the same state for the two reactions. The fact that N_2O decomposed much faster than NO, as shown in Fig. 7, indicates that the rate of oxygen desorption (Eqs. 6 and 9) is much faster than the NO decompostion, and dose not limit the rate of this reaction.

There is a possibility that the difference in the two rates shown in Fig. 7 is due to a difference of the oxidation states of the catalyst surface under the working states. The catalyst surface during the decomposition of NO would be in a more oxidized state than that during the decomposition of N_2O, since NO is a stronger oxidizing agent. Therefore, we compared the two rates simultaneously at the same oxidation states. As shown in Fig. 8, the results for the decomposition of a NO–N_2O mixture was such that the rate of the N_2O decomposition proceeded at a considerable rate, even when NO decomposition scarcely proceeded. Hence, the oxygen desorption (Eq. 6) is not rate-determining, and the rate-determining step is either NO adsorption (Eq. 4) or NO dissociation (Eq. 5), the adsorption (and desoprtion of) oxygen being in quasi-equiliblium.

The retarding effects of coexisting oxygen shown in Fig. 3 are consistent with the idea that $O_2 \rightleftarrows 2O(ad)$ is in equilibrium. TPD results also support that the desorption of oxygen is fast: The rate of oxygen desorption at 873 K in TPD of $La_{1.4}Sr_{0.6}CuO_4$ was 4.0 $\mu mol\,g^{-1}\,min^{-1}$ (Fig. 6), and greater than the rate of NO decomposition at 873 K, that is, 0.6 $\mu mol\,g^{-1}\,min^{-1}$. Thus, all the facts in the present work support that oxygen desorption is not the rate-determining step, although the reaction is retarded by oxygen that irreversibly covered the active sites (see below). This is similar to the case of the catalytic decomposition of NO over Pt/Al_2O_3 reported in the early literature.[3]

Active Sites for the Decomposition of NO.

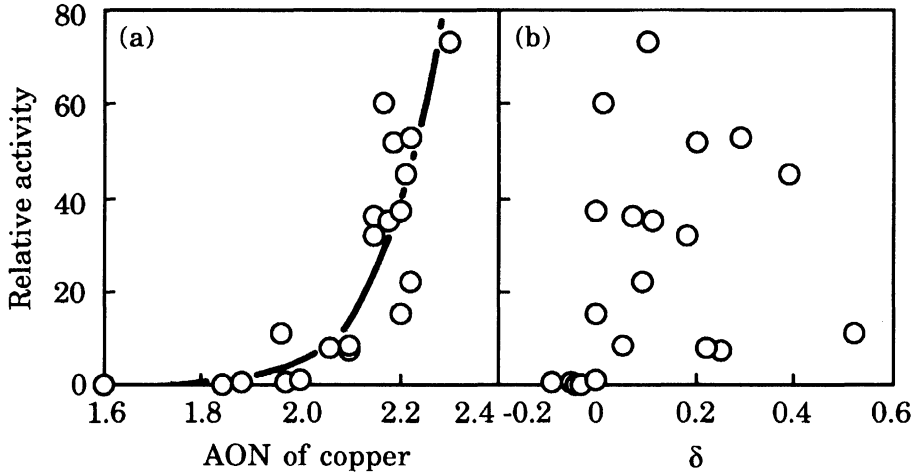

Fig. 10. Correlation between the catalytic activities of NO decomposition (1073 K) in linear scale and AON of copper (a) or δ (b) for $La_{2-x}A'_xCu_{1-y}B'_yO_{4\pm\delta}$ (see, captions in Fig. 9).

Voorhoeve[47] reported that the decomposition of NO over perovskite-type oxides proceeded at the oxygen vacancies adjacent to transition metal ions of low valency. Shin et al.[4] also reported that $SrFeO_{3-x}$ having a relatively stable oxygen-deficient structure showed significant catalytic activity.

The experiments shown in Fig. 5 (○) indicate that oxygen on the catalyst surface is partly removed by a pretreatment in He at 1073 K (cf. TPD in Fig. 6), and that NO easily dissociates on this partially reduced surface, although the rate of NO decomposition rapidly decreases as the surface is reoxidized (or covered) by oxygen produced by the decomposition. Therefore, the surface sites formed by the desorption of oxygen (surface copper ion that is coordinatively unsaturated (cus)) are active.

As shown in Fig. 1, $La_{2-x}Sr_xCuO_4$ catalysts become oxygen-deficient for $x \geq 0.4$—0.5, and the oxygen-deficiency increased with the increase of x. The amount of oxygen desorbed in TPD also tended to increase with x (see, Fig. 6 and Table 3). So the increase of catalytic activity upon the Sr substitution could be explained by the increase of cus-Cu ion on the surface. However, the catalytic activity slightly decreased for $x \geq 0.4$—0.5 (Fig. 4a). Hence, the catalytic activity can not be explained by the number of cus-Cu alone, and other factors controlling the activity must be considered.

The correlation in Fig. 9 indicates that over the entire range of x of $La_{2-x}Sr_xCuO_4$, the catalytic activity increases in general with the increase of AON. This means that the oxidation state of copper (or the redox property) is the main factor controlling the activity, although scattering of data in Fig. 9 suggests the presence of other factors. The decrease in AON of copper caused by the desorption of oxygen in TPD (298—1073 K) was only 0.04 even for $LaSrCuO_4$, for which the amount of oxygen desorbed was greatest (see, Table 3). Therefore, the changes in AON by pretreatment of reaction are not significant and the general trend in Fig. 9 should not change even if AON's under the working conditions were used for the plot.

When NO adsorbs on cus-Cu^{2+} ions, there are two possible extreme cases, viz., adsorption by Cu^+–NO^+[48] and by Cu^{3+}–NO^- (similar to Fe^{4+}–NO^-[4]):

$$Cu^{2+}(cus) + NO \rightarrow Cu^+\text{–}NO^+ \quad (10)$$

and

$$Cu^{2+}(cus) + NO \rightarrow Cu^{3+}\text{–}NO^-. \quad (11)$$

In the former, the N–O bond is strengthened and dissociation of NO becomes difficult as a result of partial electron removal from anti-bonding molecular orbital of NO. In contrast, in the latter case, the N–O bond is weakened and NO tends to easily dissociate.

If one accepts the above consideration concerning NO adsorption, the trend in Fig. 9 can be explained as follows (see Scheme 1). As discussed in the preceding section, even though Cu^{3+} in the bulk of catalyst is stable for $La_{2-x}Sr_xCuO_4$, the copper ion on the surface is Cu^{2+}. However, those Cu^{2+} ions on the surface of $La_{2-x}Sr_xCuO_4$ (x=0.2—1.0) would be more easily oxidized to Cu^{3+} upon NO adsorption than Cu^{2+} ions on La_2CuO_4 of which bulk copper ions are all Cu^{2+}. In the former case, NO would tend to adsorb by Eq. 11 and its N–O bond more easily dissociates. As a result, the rate for NO decomposition becomes fast. This explanation is consistent with the conclusion that the rate-determining step is either the adsorption or dissociation of NO. Thus, the active sites are presumably cus-Cu^{2+} ions on the surface that are easily oxidized to Cu^{3+}, and their amount and the catalytic activity increases with AON.

This mechanism reasonably explains the changes in the catalytic activities of Sr-substituted catalysts in Fig. 4a. The number of active sites (or the number of Cu^{3+}) initially increases with an increase in x. Above $x \geq 0.6$, AON (or the number of Cu^{3+}) starts to decrease,

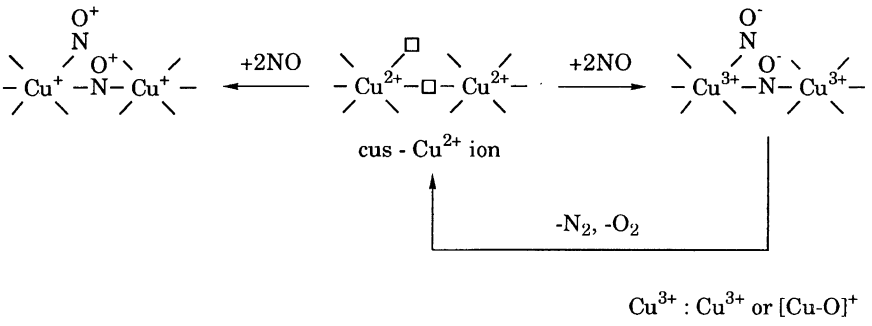

Scheme 1.

probably due to a stabilization of the oxygen-deficient structure, as discussed in the preceding section.

The relative activity of Sr-, Ba-, and Ca-substituted catalysts, i. e., Ba>Sr>Ca (x=0.2) (Fig. 4a), can be understood in a similar way. The valency of copper is controlled ($Cu^{2+} \rightarrow Cu^{3+}$) most effectively for Ba substitution owing to the highest t value (or the largest lattice energy), and hence the adsorption as Cu^{3+}–NO^- would be mostly favored. On the contrary, although the number of cus-Cu^{2+} ions (Scheme 1) on the surface is probably largest for Ca-substituted catalysts (see δ in Table 1), Cu^{3+} is least stable and the Cu^{2+} ions on the surface are not easily oxidized to Cu^{3+}, resulting in a low catalytic activity. In the case of Cu–ZSM-5, the redox cycle of $Cu^+ \rightleftarrows Cu^{2+}$ has been assumed. But in the present case, the $Cu^{2+} \rightleftarrows Cu^{3+}$ is the more probable redox cycle, as discussed above.

Comparison of Catalytic Activity of $La_{2-x}Sr_xCuO_4$ with Other Catalysts. $La_{0.8}Sr_{0.2}CoO_3$ has been reported to show the highest catalytic activity for NO decomposition among perovskite-type catalysts,[5,7] but the activity per unit surface area of $La_{1.5}Sr_{0.5}CuO_4$ in the present study is almost three times higher than that of $La_{0.8}Sr_{0.2}CoO_3$. Cu–ZSM-5 shows a significant catalytic activity for the decomposition of NO in the temperature range between 573 and 773 K.[10,11] The activities of $La_{2-x}Sr_xCuO_4$ and $La_{0.8}Sr_{0.2}CoO_3$ were not very high in this temperature range, but increased monotonically with an increase in the reaction temperature; the perovskite-type catalysts are thus more active than Cu–ZSM-5 in the high-temperature range. Since perovskite catalysts generally have a higher thermal resistance, they may possibly be applied in practical applications at high temperatures. If one considers their small surface areas, the enlargement of the surface areas, for example, by dispersing perovskites on high-surface area supports,[49] is meaningful.

Teraoka et al.,[7] reported a fair correlation between the catalytic activity for NO decomposition and that for hydrocarbon oxidation among Co- and Mn-containing perovskites and suggested the presence of a common controlling factor such as the tendency to form oxygen deficiency. However, there was no correlation between the two reactions for the present catalyst systems (Figs. 4a and 4b for Sr). Therefore, the parallelism of the two reactions observed for Co- and Mn-containing perovskites does not always hold. Hence, the essential factor controlling the activity of valency-controlled La_2CuO_4's is different between the decomposition of NO and the oxidation of C_3H_8 and the valency-control of copper is important for the former reaction.

This work was supported in part by a Grant-in Aid for Scientific Research from the Ministry of Education, Science and Culture.

References

1) J. W. Hightower and D. A. Van Leirsburg, "The Catalytic Chemistry of Nitrogen Oxides," ed by R. L. Klimisch and J. G. Larson, Plenum Press, New York (1975), p. 63.
2) A. Amirnazmi, J. E. Benson, and M. Boudart, *J. Catal.*, **30**, 55 (1973).
3) A. Amirnazmi and M. Bourdart, *J. Catal.*, **39**, 383 (1975).
4) S. Shin, H. Arakawa, Y. Hatakeyama, K. Ogawa, and K. Shimomura, *Mater. Res. Bull.*, **14**, 633 (1979).
5) T. Uchijima, *Hyomen*, **18**, 132 (1980).
6) H. Shimada, S. Miyama, and H. Kuroda, *Chem. Lett.*, **1988**, 1797.
7) Y. Teraoka, H. Fukuda, and S. Kagawa, *Chem. Lett.*, **1990**, 1.
8) H. Hamada, Y. Kintaichi, M. Sasaki, and T. Ito, *Chem. Lett.*, **1990**, 1069.
9) M. Iwamoto and H. Hamada, *Catal. Today.*, **10**, 57 (1991).
10) M. Iwamoto, "Future Opportunities in Catalytic and Separation Technology," ed by M. Misono, Y. Moro-oka, and S. Kimura, Elsevier, Amsterdam (1990), p. 121.
11) M. Iwamoto, H. Yahiro, K. Tanda, N. Mizuno, Y. Mine, and S. Kagawa, *J. Phys. Chem.*, **95**, 3727 (1991).
12) M. Iwamoto, H. Yahiro, N. Mizuno, W. X. Zhang, Y. Mine, H. Furukawa, and S. Kagawa, *J. Phys. Chem.*, **96**, 9360 (1992).
13) Y. Li and W. K. Hall, *J. Catal.*, **129**, 202 (1991).
14) Y. Li and J. N. Armor, *Appl. Catal.*, **76**, L1 (1991).
15) M. Misono, "Future Opportunities in Catalytic and Separation Technology," ed by M. Misono, Y. Moro-oka, and S. Kimura, Elsevier, Amsterdam (1990), p. 13.
16) N. Yamazoe and Y. Teraoka, *Catal. Today*, **8**, 175 (1990).
17) K. Tabata and M. Misono, *Catal. Today*, **8**, 249 (1990).

18) T. Nitadori, M. Muramatsu, and M. Misono, *Bull. Chem. Soc. Jpn.*, **61**, 3831 (1988).
19) T. Nitadori, M. Muramatsu, and M. Misono, *Chem. Mater.*, **1**, 215 (1989).
20) R. Jeyalakshmi, B. Jegannadhaswamy, K. Rengaraj, and B. Sivasankar, *Bull. Chem. Soc. Jpn.*, **63**, 2970 (1990).
21) S. Rajadurai, J. J. Carberry, B. Li, and C. B. Alcook, *J. Catal.*, **131**, 582 (1991).
22) N. Mizuno, M. Yamato, M. Tanaka, and M. Misono, *Chem. Mater.*, **1**, 232 (1989).
23) H. Yasuda, N. Mizuno, and M. Misono, *J. Chem. Soc., Chem. Commun.*, **1990**, 1094.
24) H. Yasuda, T.Nitadori, N. Mizuno, and M. Misono, *Nippon Kagaku Kaishi*, **1991**, 604.
25) K. Kishio, J. Shimoyama, T. Hasegawa, K. Kitazawa, and K. Fueki, *Jpn. J. Appl. Phys.*, **26**, L1228 (1987).
26) D. C. Harris and T. A. Hewston, *J. Solid State Chem.*, **69**, 182 (1987).
27) T. Nitadori, T. Ichiki, and M. Misono, *Bull. Chem. Soc. Jpn.*, **61**, 621 (1988).
28) J. H. Scofield, *J. Electr. Spectr. Relat. Phenom.*, **8**, 129 (1976).
29) T. Takahashi, F. Maeda, H. Arai, H. Katayama-Yoshida, S. Hosoya, A. Fujimori, T. Shidara, T. Koide, T. Miyahara, M. Onoda, S. Shamoto, and M. Sato, *Phys. Rev. B*, **B36**, 5686 (1987).
30) D. C. Frost, A. Ishitani, and C. A. Mcdowell, *Mol. Phys.*, **24**, 861 (1972).
31) G. Schön, *Surf. Sci.*, **35**, 96 (1973).
32) Y. Li and W. K. Hall, *J. Phys. Chem.*, **94**, 16 (1990).
33) T. Nakamura, M. Misono, T. Uchijima, and Y. Yoneda, *Nippon Kagaku Kaishi*, **1980**, 1679.
34) T. Nakamura, M. Misono, and Y. Yoneda, *Bull. Chem. Soc. Jpn.*, **55**, 394 (1982).
35) N. Nguyen, J. Choisnet, M. Hervieu, and B. Raveau, *J. Solid State Chem.*, **39**, 120 (1981).
36) J. B. Goodenough, G. Demazeau, M. Pouchard, and P. Hagenmuller, *J. Solid State Chem.*, **8**, 325 (1973).
37) P. Ganguly and C. N. R. Rao, *J. Solid State Chem.*,**53**, 193 (1984).
38) R. D. Shannon, *Acta Crystallogr., Sect. A*, **A32**, 751 (1976).
39) K. Sakurai, Y. Okamoto, T. Imanaka, and S. Teranishi, *Bull. Chem. Soc. Jpn.*, **49**, 1732 (1976).
40) H. Ihara, M. Hirabayashi, N. Tarada, Y. Kimura, K. Senzaki, and M. Tokumoto, *Jpn. J. Appl. Phys.*, **26**, L463 (1987).
41) P. Steiner, V. Kinsinger, I. Sander, B. Siegwart, S. Huffner, C. Politis, R. Hoppe, and H. P. Muller, *Z. Phys. B*, **B67**, 497 (1987).
42) P. Steiner, R. Courths, V. Kinsinger, I. Sander, B. Siegwart, S. Huffner, and C. Politis, *Appl. Phys.*, **A44**, 75 (1987).
43) E. R. S. Winter, *J. Catal.*, **22**, 158 (1971).
44) E. R. S. Winter, *J. Catal.*, **15**, 144 (1969).
45) H. Kobayashi and M. Kobayashi, *Catal. Rev.*, **10**, 139 (1974).
46) C. G. Takoudis and L. D. Schmidt, *J. Catal.*, **80**, 274 (1983).
47) R. J. H. Voorhoeve, "Advanced Materials in Catalysis," ed by J. J. Burton, and R. L. Garten, Academic Press, New York (1977), p. 129.
48) P. H. Kasai and R. J. Bishop, Jr., *J. Phys. Chem.*, **77**, 2308 (1973).
49) N. Mizuno, H. Fujii, H. Igarashi, and M. Misono, *J. Am. Chem. Soc.*, **114**, 7151 (1992).